

## Mitigating pulsed interference using frequency domain adaptive filtering

Mathieu Raimondi, Olivier Julien, Christophe Macabiau, Frédéric Bastide

► **To cite this version:**

Mathieu Raimondi, Olivier Julien, Christophe Macabiau, Frédéric Bastide. Mitigating pulsed interference using frequency domain adaptive filtering. ION GNSS 2006, 19th International Technical Meeting of the Satellite Division of The Institute of Navigation, Sep 2006, Fort Worth, United States. pp 2251 - 2260, 2006, <<http://www.ion.org/publications/abstract.cfm?articleID=6959>>. <hal-01021790>

**HAL Id: hal-01021790**

**<https://hal-enac.archives-ouvertes.fr/hal-01021790>**

Submitted on 31 Oct 2014

**HAL** is a multi-disciplinary open access archive for the deposit and dissemination of scientific research documents, whether they are published or not. The documents may come from teaching and research institutions in France or abroad, or from public or private research centers.

L'archive ouverte pluridisciplinaire **HAL**, est destinée au dépôt et à la diffusion de documents scientifiques de niveau recherche, publiés ou non, émanant des établissements d'enseignement et de recherche français ou étrangers, des laboratoires publics ou privés.

# Mitigating Pulsed Interference Using Frequency Domain Adaptive Filtering

Mathieu RAIMONDI, *ENAC*  
Olivier JULIEN, *ENAC*  
Christophe MACABIAU, *ENAC*  
Frederic BASTIDE, *SOFREAVIA/DTI*

## BIOGRAPHY

Mathieu RAIMONDI is a signal processing engineer. He graduated in 2005 from the ENAC in Toulouse, France. He is now a PhD Student at the ENAC and studies signal processing solutions to fight interference on GNSS receivers.

Olivier Julien is an assistant professor at the ENAC (Ecole Nationale de l'Aviation Civile), Toulouse, France. His research interests are GNSS receiver design, GNSS multipath and interference mitigation and GNSS interoperability. He received his B.Eng in 2001 in digital communications from ENAC and his PhD in 2005 from the Department of Geomatics Engineering of the University of Calgary, Canada.

Christophe MACABIAU graduated as an electronics engineer in 1992 from the ENAC in Toulouse, France. Since 1994, he has been working on the application of satellite navigation techniques to civil aviation. He received his Ph.D. in 1997 and has been in charge of the signal processing lab of the ENAC since 2000.

Frederic Bastide works as a consultant for the Direction de la Technique et de l'Innovation (DTI, ex STNA) in Toulouse. He is involved in standardization activities of future civil aviation Galileo receivers at EUROCAE level. He is also participating in Galileo system and signals standardization for civil aviation in ICAO NSP. He graduated as an electronics engineer at the ENAC in 2001 and holds a PhD in satellite navigation systems.

## ABSTRACT

Civil Aviation standardization bodies (ICAO, RTCA, EUROCAE) aim at standardizing GNSS (Global Navigation Satellite Systems) for aircraft navigation. For safety reasons, on-board receivers must guarantee integrity and accuracy performance within the specified environment. The corresponding requirements are stated

in the SARPS and MOPS (Minimum Operational Performance Specification), published by the quoted standardization bodies. Future use of Galileo E5a (or GPS L5) band raises among others interference issues. Indeed, pre-existent RF systems emit in this band, thus interfering with the E5a/L5 signals. The main threat was identified as being DME/TACAN ground beacons. These systems disturb the operation of on-board GNSS receivers in a non bearable manner if no mitigation is implemented. Two interference mitigation techniques (IMT) are proposed to fight this threat, and their performances are studied in the following. First, a baseline technique called temporal blanker is used as a reference. Its performances had already been assessed in [Bastide, 2004] and were shown to be compatible with civil aviation requirements. The idea is to detect and remove pulsed interference by looking at the signal's power. Taking into account that the input signal (in absence of interference) should be equivalent to a Gaussian noise, the user can assume with low false detection rate that if the incoming signal's power is relatively high, it is corrupted by an interference. Then, an innovative technique called Frequency Domain Adaptive Filtering (FDAF) is investigated, and is expected to provide better performance than the baseline technique. The idea is to detect and remove pulsed interference in the frequency domain by looking at the amplitude of the signal's Fourier transform because the frequency spectrum may be less distorted than the temporal signal. Nevertheless, the second technique is highly constrained by implementation issues, while the first one is not. Hence, its performance and the possible benefits brought by the technique will be presented as a function of the technique's design.

## INTRODUCTION

The future use of the Galileo E5 and GPS L5 bands raise new issues, notably concerning interference. These bands suffer concomitantly radio frequency emissions from DME (Distance Measurement Equipment), TACAN (Tactical

Air Navigation) and JTIDS/MIDS systems. These interferences disturb GNSS receivers operation for civil aviation applications, and need to be mitigated. In order to be used onboard aircrafts, the system has to show reliable performances. In the following, the study will focus on the E5a/L5 band, as this band is more impacted by pulsed interference than the E5b one. The objective is to test a technique by assessing its performance taking into account the worst case scenarios for the DME/TACAN and JTIDS/MIDS interference environment described below.

The European hot spot is defined as the place in Europe where the influence of DME/TACAN signals is the largest on the victim GNSS receivers. This scenario takes into account the emission powers and the carrier frequencies of each visible DME/TACAN ground station. The Pulse Repetition Frequencies (PRF) of each DME/TACAN emitter is considered to be set at its maximum (2700 pulse pair per second for DME and 3600 ppps for TACAN). It is supposed that from the airplane point of view, the incoming interference arrival times follow a Poisson law.

The IGEB case VIII scenario is the worst case reference scenario concerning JTIDS/MIDS signals. It does not depend on the receiver location.

The objective is to build a GNSS receiver tolerating this worst case scenarios. In this matter, two interference mitigation techniques are developed:

- The temporal blanker, whose performance was presented in previous studies. This technique is reused here and its performances are assessed in the same conditions as for FDAF.
- A frequency based technique called FDAF is proposed. Its performance are assessed and compared to the temporal blanker ones.

The Temporal Blanker performance assessment can be found in [Bastide, 2004]. It shows that GNSS receivers using the technique should comply with ICAO requirements: using the technique, no loss of lock is experienced and the C/N0 ratio stays above the minimum requirements.

Nevertheless, the number of correlators required to re-acquire the signal in case of tracking loss is very high and costly [Bastide, 2004]. Then, implementing a technique guaranteeing a higher minimum C/N0 at tracking loops input should allow to decrease the number of correlators.

Hence, FDAF is proposed as an algorithm that would guarantee higher C/N0 levels in presence of interference. Its performance is not known yet, so that there is a need to assess it, first through simulations and then, if possible, through field test.

The current paper therefore describes the interference threats before the two proposed techniques: the reference one or Temporal Blanker, and the proposed one or FDAF. Then, the implementation constraints limiting the FDAF performance will be detailed and then taken into account in the proposed simulations. Then the performances of

both techniques are compared. Finally, these have to be compared with the induced gain in the signal processing complexity.

## THREAT DESCRIPTION

The threat has been observed as being DME/TACAN ground beacons + JTIDS/MIDS. Their emissions interfere with the E5a/L5 GNSS signals, and prevent the receivers from acquiring and tracking satellites. The quoted beacons emit pulse pairs, each pulse being a Gaussian curve modulated by a cosine [Monnerat, 2000].

$$s(t) = P \times \sum_{k=1}^N \left( e^{-\frac{-\alpha(t-t_k)^2}{2}} + e^{-\frac{-\alpha(t-\Delta t-t_k)^2}{2}} \right) \times \cos(2\pi f_I t + \theta_I) \quad (1)$$

Where:

- $P$  is the DME/TACAN peak power at receiver antenna level (W),
- $\{t_k\}$  is the set of pulse pairs arrival times,
- $f_I$  is the frequency of the received DME/TACAN signal (Hz), and
- $\theta_I$  is DME/TACAN signal carrier phase at the GNSS receiver antenna port.

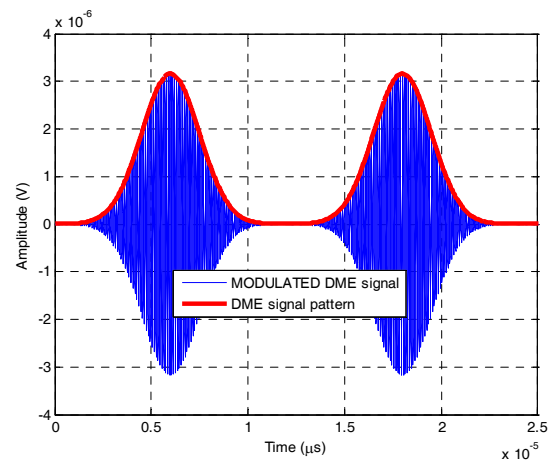


Figure 1: DME signal pattern

Figure 1 represents a DME/TACAN pulse pair. The ground stations emit up to 2700 (DME)/3600 (TACAN) pulse pairs per second (ppps). These emission rates are proper to each station.

Concerning onboard receivers, the operational environment is a combination of beacons emitting DME/TACAN + JTIDS/MIDS signals with different powers, carrier frequencies and pulse pair repetition rate. In addition, depending on the location and the Flight Level (FL) of the aircraft, each signal will suffer varying

power loss, thus will be received with different amplitudes. The exact interference configuration chosen to test the algorithm is described in the following.

### TEMPORAL BLANKER DESCRIPTION

The digital temporal blander is a simple technique, which has been studied by RTCA and EUROCAE working groups as a reference technique. It operates right after the AGC/ADC block. It assesses the power of the incoming signal and compares it to a pre-defined threshold. All the samples that exceed the threshold are considered as corrupted, and their value is set to zero (the information is removed). Figure 2 represents the transformation of a signal composed of noise and interference passed through a temporal blander.

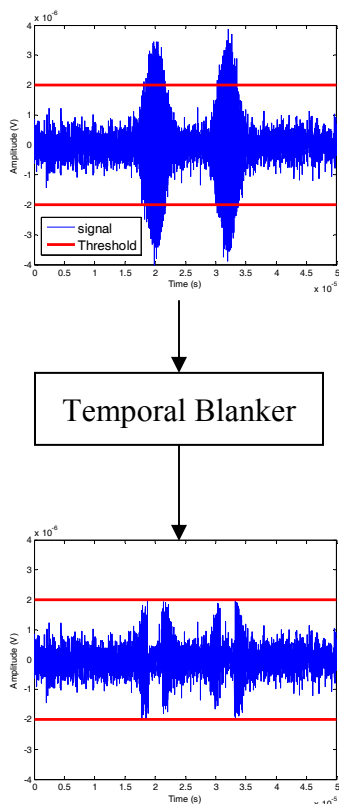


**Figure 2: Temporal Blanker Functioning**

[Bastide, 2004] assessed its performance against pulsed interference over hot spots (Europe, USA), using a simulation tool (named PULSAR) developed for the technical service of the French Civil Aviation Authority (DTI). The main criterion chosen to investigate pulsed interference mitigation techniques performance is the post-correlation Signal to Noise Ratio (SNR) degradation, as it is a common quality indicator for data demodulation, signal acquisition and tracking. The interference scenario was chosen to be the one described in the introduction of this paper for both DME/TACAN and JTIDS/MIDS signals.

[Bastide, 2004] showed that, in optimal configuration at the European hot spot, the maximum SNR degradation was around 8.9 dB in presence of DME/TACAN and JTIDS/MIDS signals, which results in a minimum post-correlation SNR very close to ICAO requirements. The technique’s performance varies with the threshold setting.

The following results were extracted from [Bastide, 2004], and take into account DME/TACAN signals. It assessed the C/N0 degradations due to interference using the temporal blander. These results were derived from a theoretical formula, and used to estimate the optimal threshold to use.

**Table 1: Temporal Blanker Performance**

Blanking Threshold (dBW)	-120	-118.4	-117.1	-115.9
Degradation (dB)	-8.9	-8.6	-8.1	-8.9

Table 1 results shows that the threshold setting can be optimized. Figure 3 shows the degradations suffered by an onboard GNSS receiver which would be flying at FL 400 (40.000 feet high over the European hot spot) using a temporal blander and setting the threshold to its theoretical optimal value determined above.

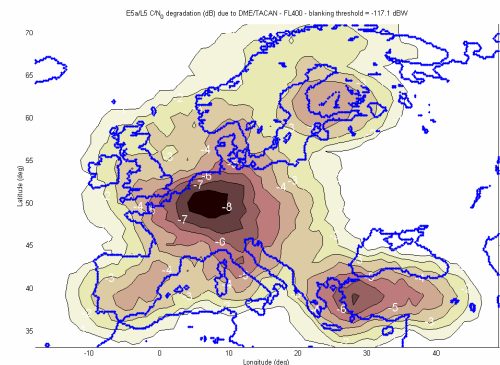


**Figure 3: Temporal Blanker against Pulsed Interference over Europe at FL 400**

Then, adding JTIDS/MIDS signal, it appears that the optimal threshold value is the same. Using the optimal value in presence of DME/TACAN and JTIDS/MIDS interference, the degradation is assessed to be equal to 8.9 dB.

### FDAF DESCRIPTION

The FDAF technique is a pulsed interference removal technique working on the frequency domain, firstly proposed in [Monnerat, 2001]. The technique works in the same place as the temporal blander, after the ADC (Analog to Digital Converter). Therefore the input of the algorithm is a quantized and sampled signal. It performs an estimation of the incoming signal’s Fourier transform, by operating a Fast Fourier Transform (FFT) on a pre-

defined number of samples ( $N$ ). It then compares the amplitude of each point of the signal's Fourier representation to a certain threshold. Note that since the incoming signal is, without disturbances, dominated by thermal noise, the FFT representation of the incoming signal should ideally be flat (white). This assumption allows the determination of a threshold that would represent the usual noise level, with a certain false alarm rate. If certain points of the incoming signal's Fourier transform exceed this threshold, they are considered corrupted by an interference and set to zero. Finally, the inverse FFT of the manipulated incoming signal is performed so as to obtain the signal back in the time domain to feed the acquisition/tracking modules. The relative narrow frequency representation of DME/TACAN signals (~1 MHz) compared to the E5/L5 GPS and Galileo signals (~20 MHz wide) allows this targeted blanking. However, note that this method might not be usable with narrow-band GNSS signals such as CW (Continuous Wave) or NBI (Narrow Band Interference) interference due to its lack of resolution.

In order not to be a computation burden, the Fourier analysis requires the incoming signal to be split into pieces composed of a determined number of samples. A large number of samples will increase the frequency resolution of the Fourier transform and would likely result into a more relevant blanking technique. However, it will also induce an increase in the computation load (FFT on an increased number of points). A trade-off between performance and computation load has then to be found.

Figure 4 details the functioning of the technique. An example of a piece of signal corrupted by a DME is passed through the FDAF.

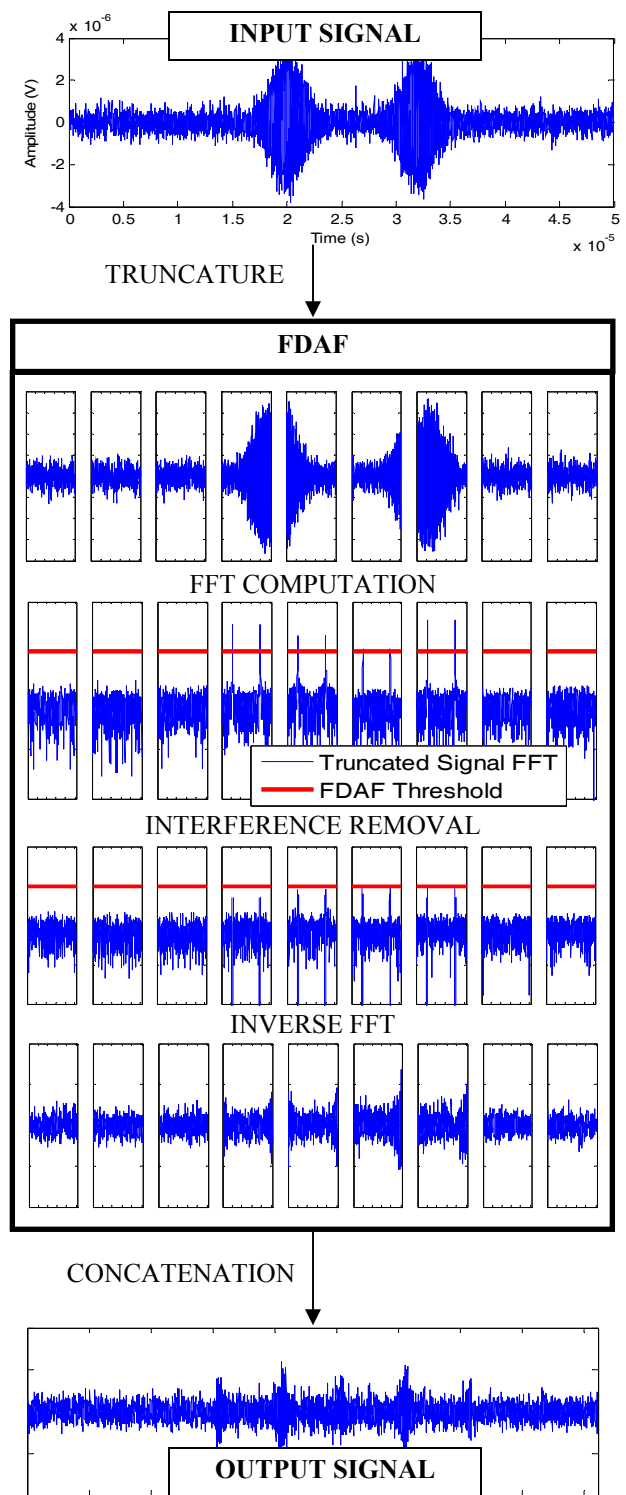


**Figure 4: FDAF Functioning Scheme**

**DECISIVE PARAMETERS SUMMARY**

The following list identifies the parameters that impact the techniques' performance, would they be constrained by implementation or not.

- The sampling frequency and the number of samples used to compute the Fourier Transform estimation ( $N$ ). These two parameters can not be separated as they determine the amount of time represented by the piece of signal processed by FDAF and the width of each channel estimated. In addition, this couple of values also determines the complexity of the technique. The number of points used to compute an FFT determines the number of operations required for its calculus, which is constrained by hardware implementation.
- The AGC/ADC block overall design. This is not intrinsic to the mitigation methods, but it modifies the processed signal, and its effects may worsen the techniques' functioning.
- The Temporal Blanker's and the FDAF threshold determination. The operation is not constrained by implementation issues, but in order to detect interference wisely, the threshold has to be above the noise floor, which is the condition to avoid false alarms. In addition, it should not be set to a very high value, in order to avoid missed detections.

### SAMPLING FREQUENCY AND FFT WINDOW SIZE ( $N$ )

General parameters such as the sampling frequency choice can not be driven by the proposed methods interests, as it impacts the entire signal processing channel. Hence, in the following it has been set to 100 MHz, as it is quite close to what could be used in future Galileo receivers.

The resolution of the estimation is determined by  $N$  and the sampling frequency. Indeed, the frequency range of the estimated Fourier Transform is constant  $\left[-\frac{f_s}{2}, \frac{f_s}{2}\right]$ ,

so the resolution is:

$$\Delta f = \frac{f_s}{N} \text{ (Hz)} \quad (2)$$

It represents the frequency spacing between two FFT channels. If the frequency interval represented by one channel is too large compared to the pulsed interference theoretical Fourier Transform, the evaluation points will not be "judicious", and the Fourier Transform may miss some interference. This is illustrated in Figure 5.

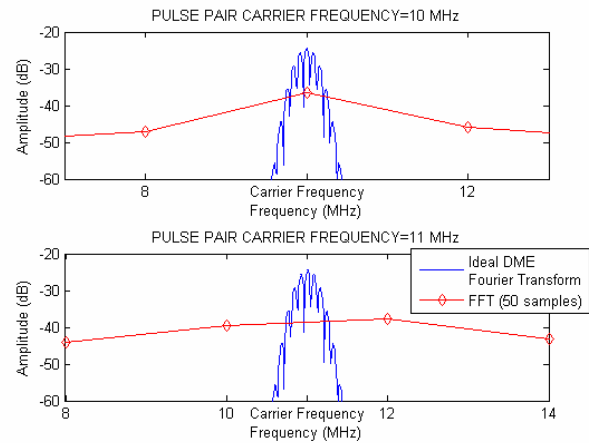


**Figure 5: FFT's Resolution and Distortion Issues ( $F_s=100$  MHz)**

The blue curve represents the theoretical Fourier Transform of a DME signal, which power is -115 dBW (typical value over the hot spot). In order to guarantee the detection of interference with a power limit, a maximum resolution can be determined. In practice, the number of points in the FFT window should guarantee at least one point in the DME bandwidth. In the here-above example, the user could wish to detect all the interference which FFT amplitude is bigger than -30 dB, what requires the resolution to be roughly thinner than 1 MHz (considering the theoretical DME frequency representation).

In the application it is not the ideal Fourier Transform that is observed, but the Discrete Fourier Transform with a limited number of points. It induces two drawbacks:

- Only a few points of the Fourier Transform represent the DME, because of the low resolution,
- The ideal curve is strongly distorted. Indeed, the Fourier transform maximum value significantly decreases and might not allow detecting pulsed interference. This is due to the averaging of the DME power contained in the frequency band represented by a Fourier transform channel.

The top figure shows that the resolution limit can not be defined easily, as the interference's FFT level depends on the number of samples used. In addition, the lower plot shows that if the interference carrier frequency is not exactly synchronised with the Frequency vector represented by the FFT, which will likely be the case in real conditions, the interference will be even more difficult to detect.

Note that the use of a rectangular window for the FFT computation will result into an estimation of each FFT frequency peak convoluted by a sinc function. This implies that the sinc side-lobes will increase the adjacent FFT channels' level and could result in their corruption. Thus it could be interesting to investigate the use of



different type of windowing to improve the FDAF performance.

This paragraph showed that it is not easy to determine the lowest resolution, because of the multiple distortions the Fourier Transform is affected by. The suffered distortions are unavoidable, but some improvements can be brought:

- The use of weighting windows before the FFT calculation would help minimizing distortions, though implying additional complexity.
- The distortions decrease when the number of points used to compute the FFT increases. Obviously, it induces additional complexity too, so a trade-off between performance and complexity is to be discussed.

### SNR DEGRADATION AS A FUNCTION OF $N$

The previous paragraphs introduced the problems that are encountered when using the technique. Hence, the number of samples used in the FFT calculation is very important in terms of performance. The following approach tries to assess how the window size impacts the performance, looking at its interference removal efficiency. In the tests, a MATLAB routine generated a signal composed of a DME pulse pair and white Gaussian noise, using a 100 MHz sampling frequency. A complete FDAF algorithm is used on this signal, and the output signal is analysed. Two test-cases are simulated to see typical FDAF behaviour in simple environment: a strong interference (high interference to noise ratio) and a much more weak interference are successively considered.

The observed performance criterion, the post correlation SNR degradation, can not be theoretically determined. Indeed, the method impacts all the signal components:

- A small part of useful signal is removed. It induces information loss.
- Thermal noise is removed too. It is not the objective of the technique but it brings benefits.
- Some of the interference is not removed.

The theoretical formula giving the degradation from the interference and the threshold used is not available. In order to roughly study the influence of increasing  $N$ , two informations are observed: the number of channels set to zero by the technique and the amount of interference that is not removed by the technique.

The interference used in the tests has a power of -102 dBW (peak power – after antenna), which is the maximum power visible over the hot spot, while the noise floor density equals -205 dBW/Hz. The threshold has been set to -118 dBW, which is just above the noise floor. Figure 6 represents, depending on time, the band filtered by the system, in Hertz. The title represents the size of the window used in samples.

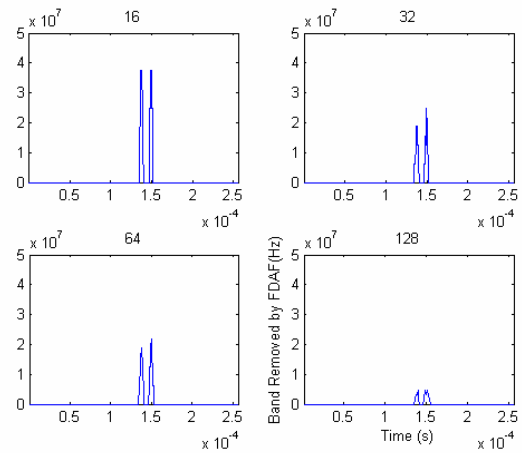


**Figure 6 : FDAF Performance Depending on the Window Size with High Interference Power**

Figure 6 shows that using small windows induces that the signal is much more filtered. This is mainly due to resolution issues. Indeed, the band removed by each concerned window should not exceed 1 MHz (2 Mhz here as the two sided FFT is considered), looking at the DME PSD. Using only 16 samples in the FDAF does not seem to fit the application, as too many channels are removed. Then, the technique’s performance increases with the window size.

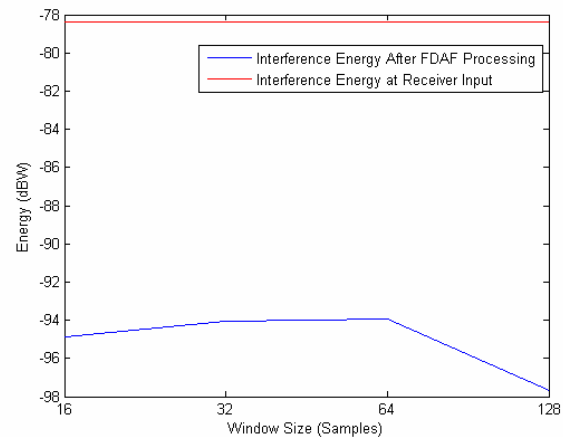


**Figure 7 : Window Size Influence on Interference Removal in case of High Interference Power**

Figure 7 represents the efficiency of the technique on removing the present interference as a function of the FFT window size. Apparently, the efficiency of the technique does not grow systematically with the window size. Indeed, when increasing the number of samples, the noise floor grows faster than the interference peak, so that detection becomes more and more difficult. Due to the high threshold choice, the left interference presents high energy.

In the next test, the same noise (noise floor density equals -205 dBW/Hz) and threshold have been used, but the interference power has been severely decreased (-126 dBW). This is the minimal power observable over the hot spot.

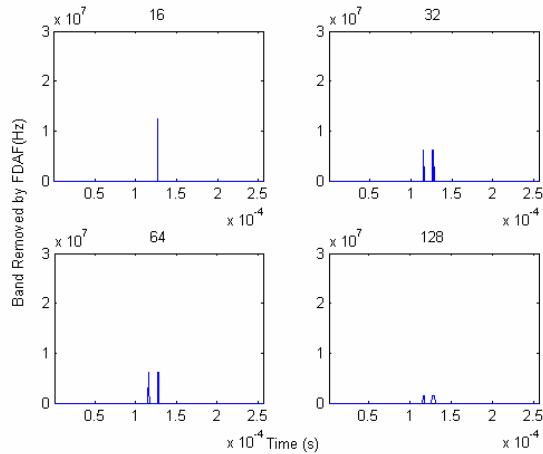


**Figure 8: FDAF Performance Depending on the Window Size with Low Interference Power**

Figure 8 shows the efficiency of the technique depending on the window size. Using too small window will induce missed detections, and when the interference is detectable, the increase of the window size helps removing less signal.

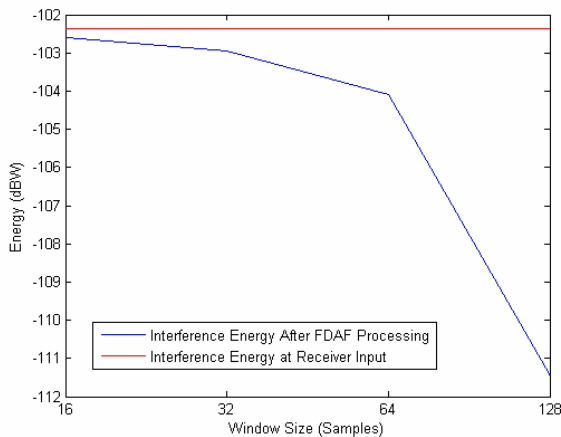


**Figure 9 : Interference Power Removed by the Technique depending on the Window Size in case of Low Interference Power**

Figure 9 shows the power of the interference removed by the technique depending on the window size. The removed part of the pulse pair highly varies over the window size and in the shown range, the best option is to increase it as much as possible.

## AGC/ADC IMPLEMENTATION

The quantization process is a source of additional error, often considered as an additive noise:

$$signal_Q = signal + noise_Q \quad (3)$$

This noise is assumed to be white and Gaussian. It induces small SNR degradations, which can be calculated from the quantization law, the number of bits used, and the signal's standard deviation, as shown in Figure 10 (extracted from [Bastide, 2004]).

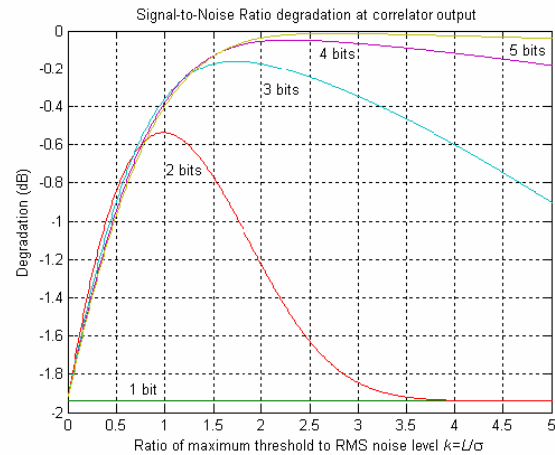


**Figure 10: SNR degradation at correlator output in presence of thermal noise only**

The presented results were obtained assuming thermal noise only enters the ADC.

The SNR degradation is represented at correlator output and depends on a variable  $k$ .  $k = \frac{L}{\sigma}$ , where  $L$  is the maximum quantization level (saturation level), and  $\sigma$  is the input signal's standard deviation.

The degradation depends on the number of bits used in the converter, so that several curves obtained using various numbers of bits are presented on the figure.

For each curve, there is an optimal  $k$  for which the quantization loss is minimal. As stated above,  $k$  depends on the maximum quantization level ( $L$ ), which only depends on  $N$  (the number of bits) and the quantization step ( $\Delta$ ), and the input signal's standard deviation ( $\sigma$ ). The role of the AGC is to force the output signal's standard deviation to a constant value, by multiplying it by a gain. This stage is primordial for optimal ADC functioning, as it will keep the signal's standard deviation and so the variable  $k$  to the optimal value.

The AGC gain is calculated by looking at the ADC output signal. Analyzing its statistics or its power, the AGC applies the gain that optimizes quantization. Usually, this



is performed assuming that Gaussian noise only is present (GNSS signal is negligible at this stage). In presence of interference, three issues are raised:

- The AGC functioning is disturbed. It estimates the standard deviation, which is corrupted by interference,
- The ADC's input signal does not follow a Gaussian distribution. Figure 10 results are not valid anymore.
- The modification of the signal (notably interference) may worsen the IMT's efficiency.

To solve the AGC problem, the signal is observed at interference mitigation techniques' output instead of ADC's output. In this way, the observed signal can be assumed as interference free, so that the standard deviation estimation is valid.

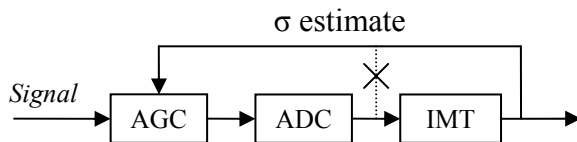


Figure 11: AGC Steering Mode

In addition, Figure 10 results were obtained considering noise only at the ADC's input, which is not the case when interference is present. The major concern is to avoid saturation, as interferences are assumed to present higher power than ambient noise.

This problem can be solved by using a great number of bits and adapting the AGC functioning. It is set to regulate the signal to optimize a 3 bit quantizer. This is illustrated in Figure 12.

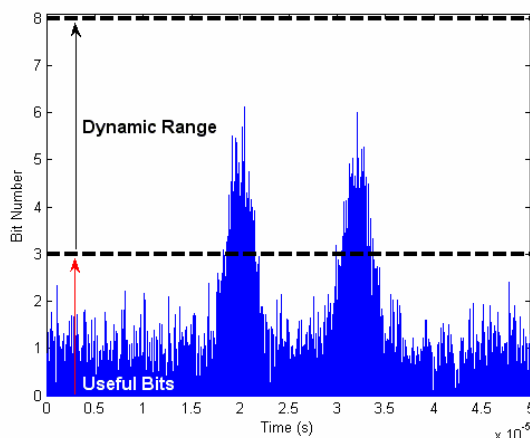


Figure 12: AGC/ADC implementation

Nevertheless, the number of bits used in the ADC is constrained by implementation. Increasing the number of bits implies better performances, but increases the ADC's cost too.

The last problem is the quantization impact on IMT's functioning. Concerning the temporal blanker, it is supposed to be less accurate than considering continuous signal. Nevertheless, the technique has been studied to process digital and not analog signals. It does not fundamentally disturb the technique.

FDAF does not suffer the implementation of a quantizer, as it preserves the interesting properties of the signal. Thanks to the model proposed by (3), the ADC's output signal can be considered as the sum of the pre-existing signal (GNSS signal + interference + thermal noise) and quantization noise, which is white. It means that the FDAF input signal has the same properties, but the noise level is slightly higher.

$$\begin{aligned} FFT(signal_o) &= FFT(signal + noise_o) \\ &= FFT(signal) + FFT(noise_o) = FFT(signal) + c \end{aligned} \quad (4)$$

Where c is a constant.

## IMT'S THRESHOLD DETERMINATION

### TEMPORAL BLANKER THRESHOLD

In [Bastide, 2004] tests, the technique shows optimal performance using a threshold value equivalent to -117.1 dBW. Indeed the observed signal is quantized, and thus the threshold is digital too. This means that the threshold is set to one of the quantization level. The equivalent analog threshold can then be calculated according to the AGC gain applied to the signal.

In [Bastide, 2004], and in the simulations realized in this document, the noise density power level is supposed constant and equal to -205 dBW/Hz, and thus the AGC optimal gain can be calculated easily. Over the European hot spot, the best performance, represented by the minimal post-correlation  $C/N_0$  degradation, was reached by setting the threshold to 8 (digital domain – the equivalent value in the analog domain is given in Table 2). Knowing the gain applied (assumed constant and optimal in these tests), it is possible to determine the equivalent analog threshold through:

$$Th_{analog} = 20 \times \log_{10} \left( \frac{Th_{digital} - 1}{G} \right)$$

However, in real case application, the noise floor is expected to slowly vary with time, and so is the gain. Then, a constant quantization level will not represent exactly the same power.

**Table 2: Digital/Analog Threshold Conversion**

Digital Threshold	Noise floor	AGC Gain	Analog Threshold
8	-205 dBW/Hz	4.88*1 <sup>6</sup>	-116.87 dBW
	-200 dBW/Hz	2.74*1 <sup>6</sup>	-111.85 dBW

Table 2 shows that if the noise floor increases, the technique will let more interference pass.

In this report, a slightly different case will be taken: the simulations will be run using an adaptive AGC. The threshold will be determined depending on the number of bits and the quantization law chosen in the ADC.

### FDAF THRESHOLD DETERMINATION

In order to wisely choose the threshold, the observed estimator (FFT) can be expressed as a function of a Power Spectrum Density (PSD) estimator, the periodogram, which statistical properties are known.

$$Periodogram = \frac{|FFT|^2}{N} \Rightarrow FFT = \sqrt{N * Periodogram} \quad (5)$$

The objective is to distinguish pulsed interference from white noise. The characteristics of the white Gaussian noise periodogram are:

$$\begin{aligned} \mu_{perio} &= \sigma_{noise}^2 \\ \sigma_{perio}^2 &= \sigma_{noise}^4 \end{aligned} \quad (6)$$

For quantization losses optimization purpose, the AGC/ADC block outputs a signal with constant and known variance (considering no interference is present). So at the FDAF input, the noise variance is supposed to be equal to 3.39. Knowing the mean and the variance of the estimator, and assuming that the estimations follow a Gaussian law, it is possible to determine the range the PSD estimations lie in. It can be assumed that the estimator (the periodogram) will not exceed the following value:

$$\mu_{perio} + 3 \times \sigma_{perio} = \sigma_{noise}^2 + 3 \times \sigma_{noise}^4 \quad (7)$$

This could be used as a threshold considering the periodogram. In the present case, the estimator is the FFT, which is linked to the periodogram by relation (5).

$$\begin{aligned} Perio \leq Threshold_{perio} &\Rightarrow FFT \leq \sqrt{N \times Threshold_{perio}} \quad (8) \\ &\Rightarrow FFT \leq \sqrt{N \times (\sigma_{noise}^2 + 3 \times \sigma_{noise}^4)} \end{aligned}$$

In the following tests, the threshold has been set using this expression. Even if it is not the optimal value, the chosen threshold should be a good trade-off between signal loss and interference detection, according to thermal noise statistical properties.

### SIMULATOR DESCRIPTION

The performances of the techniques were obtained using a software simulator called PULSAR. The simulator is developed under Labview and is composed of:

- A signal generation block. This block generates an E5a signal, thermal noise, and pulsed interferences.
- A signal processing block composed of a front end filter, an AGC/ADC, different IMT and correlators.
- A tracking loop.

Then, a C/N0 estimator provides its value at correlation output. The carrier to noise density is calculated using the following formula :

$$\frac{C}{N_0} = \frac{E[I_p]^2}{Var[I_p]} \times B_{PD} \quad (9)$$

Where:

- $I_p$  are the prompt Inphase samples,
- $B_{PD}$  is the PreDetection Bandwidth.

The number of samples used to compute the mean and the variance of the signal are defined by the smothering length (user command). The predetection bandwidth is the inverse of the predetection integration time, which is the time required to output one correlator sample.

Then, each carrier to noise density ratio is passed through an averaging filter using four values.

### SIMULATION SIGNAL ENVIRONMENT

The simulations were run using a QPSK modulated L5 code. Its reception power has been set to -155 dBW. The noise is a white Gaussian noise (Labview function) and its density equals -200 dBW/Hz. The pulsed interferences were generated using the theoretical expression given above. The objective being to test the techniques in worst cases scenarios, the simulation occurs over the European

hot spot. In the simulator, the hot spot is defined by a table of frequencies, pulse repetition rates and powers, which is extracted from the Galileo interim MOPS. Then, a Matlab routine generates the arrival times of the DME signals using a Poisson law.

### SIMULATION RESULTS

Three tests were conducted:

- A first one using the temporal blanking as a mitigation technique. It is used as a baseline of what is achievable today.
- Two others using FDAF, with different settings. The first one used 128 samples for each Fourier Transform estimation, the second one only 64. The latter is expected to show worse performance than the previous one, but less complex too.

**Table 3: Simulation Results**

IMT Used	Post Correlation SNR Degradation
Temporal Blanker	<b>10 dB</b>
FDAF 128 (1920 operations)	<b>4 dB</b>
FDAF 64 (832 operations)	<b>6.6 dB</b>

With the considered settings, FDAF shows better performance than the temporal blanker. In addition, the 128 samples FDAF performs better than the 64 samples FDAF, what was expected. The gain is of about 2.5 dBs, which may justify the increase of complexity. It is possible to use even more samples in the Fourier Transform estimation (256, 512...) but the corresponding performance increase may not be significant enough. A trade-off has to be done between performance and complexity.

It is to be noticed that the degradation estimated using the Temporal Blanker is different from the one obtained in the reference [Bastide, 2004]. The simulator has been slightly modified: the front end filter was simplified while the quantization block and the sampling frequency were modified. This should justify the 1 dB difference between the upper tests and the reference ones.

### CONCLUSION

The FDAF definitely shows better performance than the Temporal Blanker. It has been seen that the latter technique is costless compared to FDAF and already complies with ICAO requirements. Nevertheless, implementing FDAF with a 64 samples wide window results in a 6.6 dB C/N0 degradation compared to a 10 dB degradation over the European hot spot. Therefore FDAF brings an improvement of the signal's quality, probably allowing reducing the complexity of further signal processing. Following work should be to compare the

complexity gain brought by the technique to the additional calculation effort required to implement it.

### ACKNOWLEDGMENTS

This work has been done for the ANASTASIA project. This project is financed CE DG Research in the framework of the 6<sup>th</sup> PCRD.

### REFERENCES

[Bastide et al.,2003], Bastide, F., D. Akos, C. Macabiau, and B. Roturier: *Automatic Gain Contron (AGC) as an Interference Assessment Tool*, ION GPS 2003.

[Bastide,2004], Bastide, F.: *Analysis of the Feasibility and Interests of Galileo E5a/E5b and GPS L5 Signals for Use with Civil Aviation*, PhD. Thesis.

[Monnerat, 2000], Monnerat M., B. Lobert, S. Journo, C. Bourga : *Innovative GNSS2 navigation signal*, Proceedings of the Institut of Navigation GPS meeting, Salt Lake City, UT, September 2000.

[GALILEO\_MOPS]: Interim Minimum Operational Performance Specification For Galileo Satellite Positioning Receiver. Eurocae WG-62 works

[Monnerat, 2001]: Monnerat M., Erhard P., Lobert B.: *Performance Analysis of a GALILEO Receiver Regarding the Signal structure, Multipath, and Interference Conditions*, ION GNSS 2003.

[Bastide, 2004]: Galileo E5a/E5b and GPS L5 acquisition time statistical characterization and application to civil aviation, ION GNSS 2004